# EXPERIMENTAL STUDIES ON THE ROLLING EFFECT ON HEAT LOSSES FROM OIL TANKER CARGOES

Suhara, Jiro
Faculty of Engineering, Kyushu University : Professor

Kato, Hiroharu
Faculty of Engineering, University of Tokyo : Associate Professor

Kurihara, Tomomichi
Technical Research Institute, Hitachi Shipbuilding & Engineering Co. , Ltd. : Research Engineer

https://doi.org/10.5109/6610199

出版情報：Reports of Research Institute for Applied Mechanics. 24 (76), pp.1-30, 1976-07. 九州大学応用力学研究所
バージョン：

Reports of Research Institute for Applied Mechanics
Vol. XXIV, No. 76, 1976

# EXPERIMENTAL STUDIES ON THE ROLLING EFFECT ON HEAT LOSSES FROM OIL TANKER CARGOES

By Jiro SUHARA,* Hiroharu KATO**
and Tomomichi KURIHARA***

Experimental studies were carried out on the rolling effect upon heat transfer through the shell plating of an oil tanker. The results obtained are as follows:

(1) Increment in the heat transfer coefficient for the shell plating by rolling of ship was investigated using a 1/50 size model and the following empirical formulae were obtained.

For side shell plating: $\Delta Nu = 0.0160\ Re^{0.942} Pr^{1/3}$

For bottom shell plating: $\Delta Nu \cong 0.0155\ Re^{0.910} Pr^{1/3}$

(2) The experimental results obtained by the test on an actual ship are reasonably and well explained using the empirical formulae mentioned above.

(3) Increment in heat transfer by rolling of ship is mainly caused by the stirring effect of stiffeners.

## 1. Introduction.

It is often needed, especially in winter, to heat up cargo oil for improving its dischargiability and heating coils are usually installed at the bottom of tanks for the purpose.

Recently, several reports are published on heat transfer through the shell plating of tankers and that from the heating coil [1)~3)]. By using these data more reasonable design of heating coil system has become possible. However, some important problems have yet been left out of consideration. One of which is the effect of rolling of ship on heat transfer through the shell plating.

This paper reports an experimental study on the subject. Experiments of model as well as actual ship were carried out.

* Professor. Faculty of Engineering, Kyushu University
** Associate Professor, Faculty of Engineering, University of Tokyo
*** Research Engineer, Technical Research Institute, Hitachi Shipbuilding & Engineering Co., Ltd.

## 2. Preliminary Experiment

### 2.1. Experiment on the stirring effect by stiffeners

The heat losses from the shell plating when ship is rolling, can be expressed as follows:

$$Q = [(\alpha+\Delta\alpha)A+(\alpha_f+\Delta\alpha_f)A_f\,\phi](\theta_\infty-\theta_w) \tag{1}$$

where $\Delta\alpha$ and $\Delta\alpha_f$ are the increment of the heat transfer coefficient by rolling for the shell plating and for the stiffener, respectively.

A series of tests using part models of the shell plating with stiffeners, one of which is shown in Fig. 1, were carried out so as to know the rough amount of $\alpha$, $\alpha_f$, $\Delta\alpha$ and $\Delta\alpha_f$. An electric heater is mounted behind the shell plating and the backside of the model is insulated in order to reduce the heat loss from that side. Therefore, the direction of the heat flow in the model tests is reverse to the actual condition. The model is set up in the test tank filled with oil and oscillated longitudinally with a crank mechanism driven by an electric motor.

The principal items of the models tested are shown in Table 1. Plastic stiffeners were prepared to make comparison with brass ones; the thermal

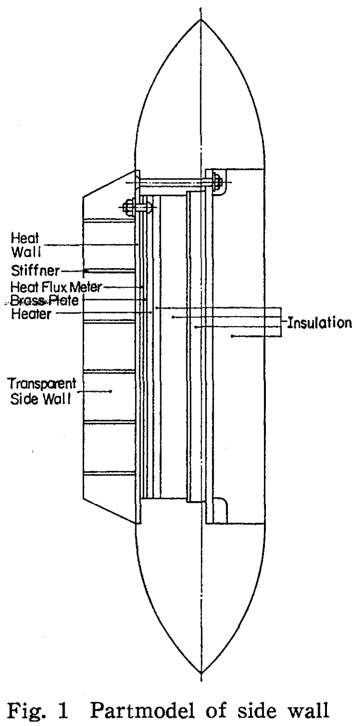


Fig. 1 Partmodel of side wall

conductivity of the former is much less than that of the latter. As test oil, kerosene and high viscosity oil (SHELL ONDINA OIL) were used.

The amplitude and the frequency of oscillation were chosen so as to correspond to those of actual ship. The temperature of the shell plating and the bulk oil were measured with copperconstantan thermocouples and the heat flux with heat flux meters specially made by one of the authors. Details of the heat flux meter are mentioned in the appendix.

Test results are shown in Fig. 2. The heat transfer coefficients were analyzed using the area of the heating surface without stiffeners. From Fig. 2, it became clear that:

(1) The heat transfer coefficient is increased by rolling. The increment is correspond to the magnitude of the amplitude and the frequency of rolling.

Table 1 Type of stiffener

| | | | |
|---|---|---|---|
| Side Wall | Material : Brass<br>Size (mm) : $140\times100\times2$<br>No. of Stiffener : 6 | | |
| Stiffener | A | B | C |
| Material | Brass | Brass | Plastic |
| Height (mm) | 10 | 20 | 20 |
| Thickness (mm) | 0.75 | 0.75 | 1.02 |
| Space (mm) | 20 | 20 | 20 |

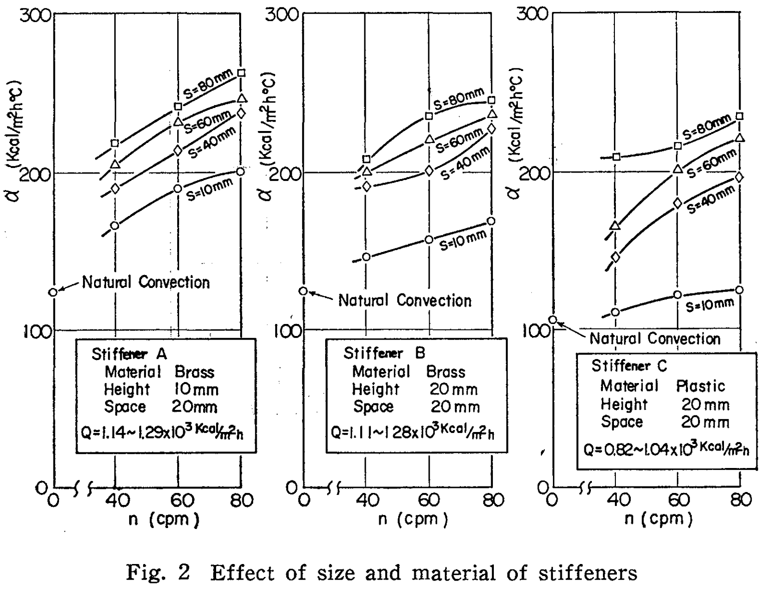


Fig. 2 Effect of size and material of stiffeners

(2) The height and the thermal conductivity of the stiffener do not affect so much on the heat transfer coefficient.

(3) It is interesting that the shorter stiffener ($k = 10$ mm) shows a little better heat transfer than the taller one ($k = 20$ mm).

The stiffener is considered to be a fin in the heat transfer problem. The efficiency of a rectangular fin is calculated by the following equation.

$$\phi = \tanh Z/Z \tag{2}$$

where

$$Z = k\sqrt{\frac{2\alpha_f}{\lambda d}}$$

Thus, the apparent fin efficiency $\Psi$ of a plating with stiffeners can be defined as follows:

$$\Psi = 1 + \frac{\alpha_f A_f}{\alpha A}\phi \tag{3}$$

The calculated results of $\Psi$ for the test models are shown in Fig. 3. In the calculation, the thermal conductivities of brass and plastic are assumed to be 95 and 0.2 kcal/mh°C, respectively, and the surface heat transfer coefficient of the shell plating 100 kcal/m²h°C.

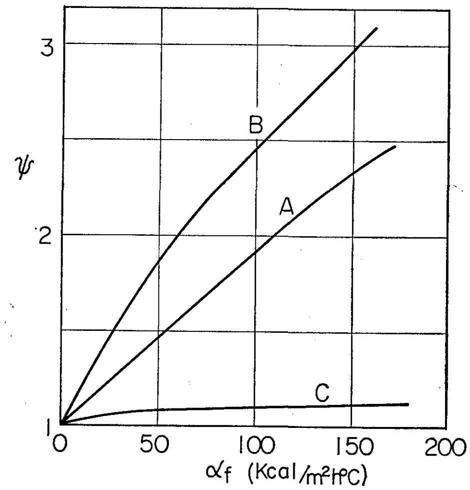


Fig. 3 $\Psi$ of Stiffener

As seen in Fig. 2, the apparent heat transfer coefficient based on the net area of the shell plating changes little in spite of a great change both in the size and the thermal conductivity of the stiffener. This fact means the

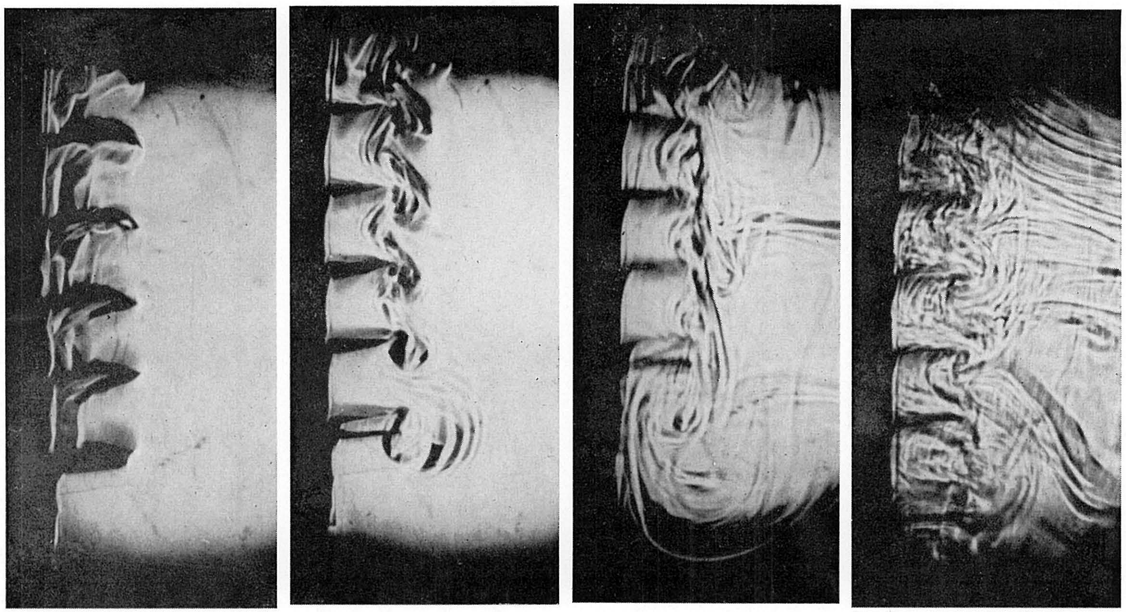

(a)
S = 0 mm
T = ∞ sec
(Natural Convection)

(b)
S = 10 mm
T = 1 sec

(c)
S = 40 mm
T = 1.5 sec

(d)
S = 40 mm
T = 0.75 sec

Photo 1 Observation of flow by shadowgraph method apparent heat transfer coefficient of the shell plating is little affected by the stiffeners. If it is not so, the model with stiffener B should show the greatest value and the magnitude of the values obtained for the model with stiffener A or B and that with C should be reverse. Thus, as the first approximation, the efficiency of the stiffener $\Psi$ can be considered as unity. Then, the equation (1) is reduced to as follows:

$$Q = (\alpha + \Delta\alpha)(\theta_\infty - \theta_w)A \qquad (4)$$

### 2.2. Observation of the fluid flow in a tank

The shadow-graph method was used to observe the fluid motion near the shell plating. As seen in Photo 1, the stirring effect is most violent around the edge of stiffeners. It is also cleared by observation that, when the stiffener is taller than a certain limit, the stirring effect does not reach to the surface of the shell plating and the heat transfer decreases as the result. On the other hand, when the height of the stiffener is reduced too much, the stirring effect on the shell plating decreases and the heat transfer also decreases as the result. Therefore, there must be a suitable height of the stiffener that gets the maximum stirring effect and the maximum heat transfer.

## 3. Tank Model Experiments

A one-fiftieth-scale cargo wing tank model of a standard 150,000 DWT tanker was used. Because the heat loss from a wing tank is much greater than that from a center tank and the rolling effect is expected to be dominant at the side shell plating. The dimensions and the other items of the model are shown in Table 2. The rolling period in the model experiments

Table 2 Comparison between ship and model

| Item | | Ship | | Model (1/50) | |
|---|---|---|---|---|---|
| Size (m) | Tank : B×D | 10×20 | | 0.2×0.4 | |
| | Stiffener : k×l | 1×1 | | 0.02×0.02 | |
| Rolling Angle (deg) | | 0∼15 | | Do. | |
| Rolling Period (sec) | | 10, 20 | | 1.43, 2.86 | |
| (where $\frac{\text{Rolling Period}}{\text{Period of Natural Freq. of Free Surface}} = \text{const.}$) | | | | | |
| Fluid & $\nu$(cm²/sec) at 30°C | | Name | $\nu$ | Name | $\nu$ |
| | | B-Heavy Oil | 1.40 | Water | $0.80\times10^{-2}$ |
| | | C-Heavy Oil | 20.9 | Kerosene | $1.36\times10^{-2}$ |
| | | | | Ethylene Grycol | $12.2\times10^{-2}$ |

was determined so as to keep constant the ratio defined and described in the above-mentioned table. Therefore, the Reynolds number of the model could be equalized to that of the actual ship by using a fluid with lower viscosity than crude oil. In order to satisfy the condition, water, kerosene and ethylene grycol were used in the experiment.

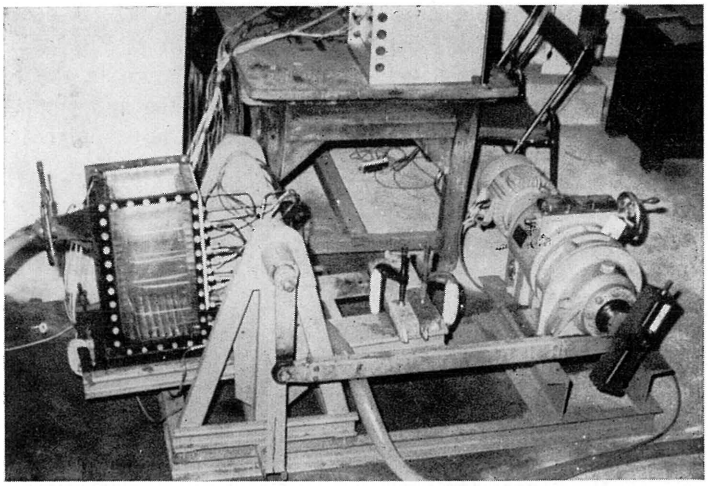

Photo 2 Test rig

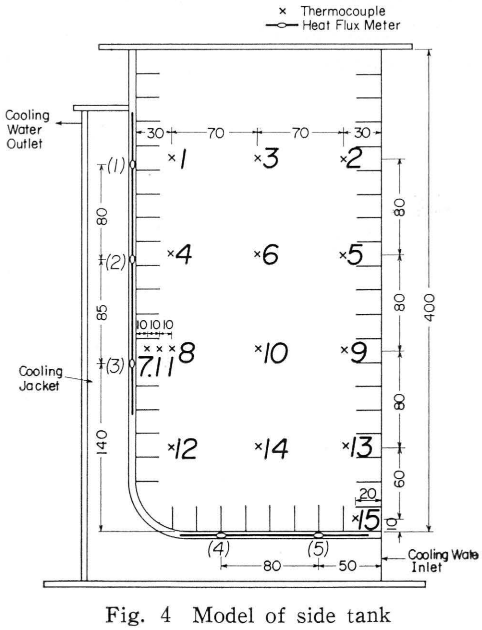


Fig. 4 Model of side tank

### 3.1. Apparatus

The model and the rolling test rig are shown in Photo 2. The wing tank model is set at the position corresponding to the relative position of the wing tank in the actual tanker. The rolling amplitude and frequency of the test rig can be controlled arbitrarily by a crank device and a variable-speed electric motor. The two transverse walls of the model are transparent plastic plates in order to observe the fluid flow inside the tank. A cooling jacket is fitted at the bottom and side shell plating as shown in Fig. 4. The position of thermocouples and heat flux meters is also shown in the figure.

The shell plating is composed of doubled brass plates and five thermocouples and five heat flux meters are installed between the two plates. A 2-KW sheathed electric heater is set near the bottom of the tank for the purpose of heating up the test fluid.

### 3.2. Effect of rolling

Fig. 5 shows an example of test results. The fluid in the tank was heated up to a certain temperature and left as it is for an hour. After that rolling motion was applied. There was some temperature difference in the fluid initially, but it became little rapidly by rolling. The heat transfer coefficients were analyzed using the bulk temperatures indicated by the following thermocouples:

| | | | | |
|---|---|---|---|---|
| Thermocouple | No. 1 | for | Heat flux meter | No. 1 |
| Do. | No. 4 | for | Do. | No. 2 |
| Do. | No. 12 | for | Do. | No. 4 |
| Do. | No. 13 | for | Do. | No. 5 |

(Heat flux meter No. 3 was damaged)

The following matters became evident after examining the experimental results.

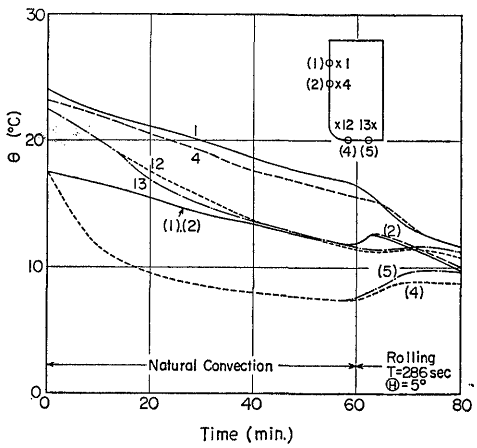


Fig. 5 Rolling effect on heat transfer (Water)
(a) Temperature

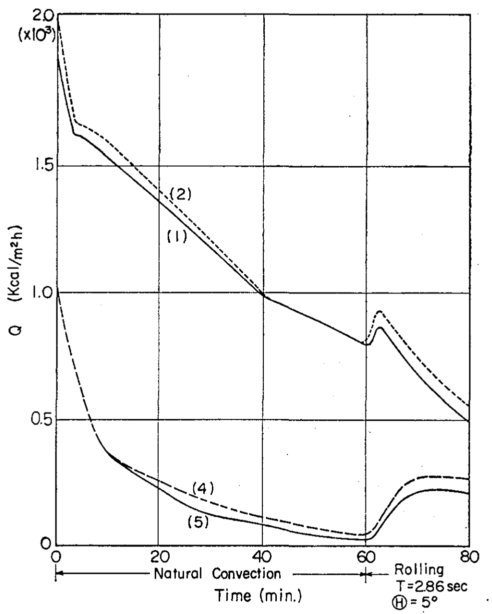


Fig. 5 Rolling effect on heat transfer (Water)
(b) Heat Flux

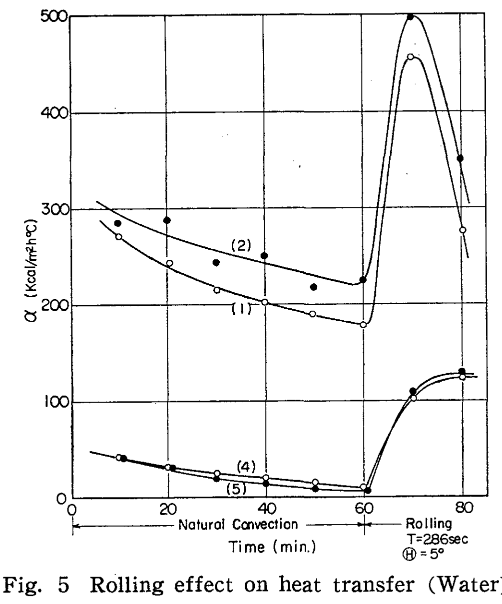


Fig. 5 Rolling effect on heat transfer (Water)
(c) Heat transfer coefficient

(1) For cooling without rolling

(a) The bulk temperature differs much vertically, but little horizontally.

(b) The heat transfer coefficient at the side shell plating agrees well with the calculated value according to the following formula for the vertical natural convection:

$$Nu = 0.56(Gr \cdot Pr)^{1/4} \tag{5}$$

(c) The heat transfer coefficient at the bottom shell plating is about 10 percent of that at the side shell plating, and the value agrees with the calculated one based on the assumption that the heat transfer is dominated by heat conduction only.

(2) For cooling with rolling

(a) The bulk temperature becomes uniform rapidly after rolling begins.

(b) The heat flux as well as the heat transfer coefficient is increased by rolling, and it is especially remarkable at the bottom. They take maximum values immediately after rolling begins. This arises from the stirring effect conveying hot fluid at the center of the tank to the cold shell plating. It is very interesting that the above-mentioned fact is also observed in the test by the actual ship, as to be mentioned in paragraph **4.2.**.

### 3.3. Fluid motion in a tank

The heat transfer from the side and the bottom shell platings and the thermal diffusion in the fluid are significantly affected by the rolling motion of ship. So the authors tried some theoretical consideration on the fluid motion in the tank.

In order to simplify the calculation, we assume that the fluid is non-viscous and the surfaces of the tank wall are flat. Then the motion of the fluid in a rectangular tank is calculated by applying the potential theory. The co-ordinates and symbols are shown in Fig. 6.

Let the ship roll around its origin 0 according to Eq. (6).

$$\theta = \Theta \sin \omega t \tag{6}$$

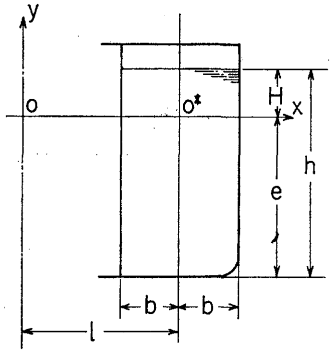


Fig. 6 Coordinates and symbols

Then, using the velocity potential $\phi$, the motion of the fluid in the tank and the boundary conditions can be expressed as follows:

$$\nabla^2\phi = 0 \tag{7}$$

$$u = -\frac{\partial\phi}{\partial x},\quad v = -\frac{\partial\phi}{\partial y} \tag{8}$$

$$(1)\quad x = \pm b,\ \frac{\partial\phi}{\partial x} = \Theta\omega y \cos\omega t \tag{9}$$

$$(2)\quad y = -e,\ \frac{\partial\phi}{\partial y} = -\Theta\omega(x+l)\cos\omega t \tag{10}$$

$$(3)\quad y = H,\quad \frac{\partial^2\phi}{\partial t^2} = g\frac{\partial\eta}{\partial t} = -g\frac{\partial\phi}{\partial y} \tag{11}$$

Taking for $\phi$ the expression

$$\phi = \phi_1(x,y)\cos\omega t \tag{12}$$

we obtain the following boundary conditions for $\phi_1$.

$$x = \pm b,\ \frac{\partial\phi_1}{\partial x} = \Theta\omega y \tag{9$'$}$$

$$y = -e,\ \frac{\partial\phi_1}{\partial y} = -\Theta\omega(x+l) \tag{10$'$}$$

$$y = H,\ \omega^2\phi_1 = g\frac{\partial\phi_1}{\partial y} \tag{11$'$}$$

By writing $\phi_1$ in the form of Eq. (13)

$$\begin{aligned}\phi_1 = {}& \Theta\omega(xy - ly + lH - \frac{g}{\omega^2}l)\\ &+\sum_m A_m \sin m\alpha x \cosh m\alpha(y+e)\\ &+\sum_m B_m \sin m\alpha x \cosh m\alpha(H-y)\end{aligned} \tag{13}$$

where $A_m$, $B_m$ are some constants and $m = 1, 2, \cdots\cdots$, we satisfy the laplacian equation (7).

The substitution of Eq. (13) in Eqs. (9)$'$, (10)$'$ and (11)$'$ gives

$$A_N = \frac{\Theta\, C_N\left(g - \omega^2 H - \dfrac{4b\omega^2}{\pi N \sinh\frac{\pi Nh}{2b}}\right)}{\omega\cosh\frac{\pi Nh}{2b} - \frac{\pi g N}{2b}\sinh\frac{\pi Nh}{2b}}$$

$$B_N = \frac{2\Theta\ \omega C_N}{\frac{\pi N}{2b}\sinh\frac{\pi Nh}{2b}}$$

where

$$m\alpha = \frac{\pi}{2a}(2n+1)$$

$$N = 2n+1,\quad n = 0,\ 1,\ 2,\ \cdots\cdots$$

$$C_N = C_{2n+1} = \frac{8b(-1)^n}{(2n+1)^2\pi^2}$$

Taking into account the first term of series for the approximation, we obtain

$$\phi = \Theta\omega\ \cos\ \omega t\Big[xy-ly+lH-\frac{g}{\omega^2}l$$

$$+\frac{8b\left\{g-\omega^2(H+\frac{4b}{\pi S})\right\}}{\pi^2(\omega^2C-\frac{\pi g}{2b}S)}\sin\frac{\pi x}{2b}\cos h\frac{\pi(y+e)}{2b}$$

$$+\frac{32b^2}{\pi^3 S}\sin\frac{\pi x}{2b}\cosh\frac{\pi(H-y)}{2b}\Big] \tag{14}$$

where

$$C\equiv\cosh\frac{\pi h}{2b},\quad S\equiv\sinh\frac{\pi h}{2b}$$

Thus, the relative tangential velocity of the fluid at the surface of the side and the bottom shell platings are given as follows:

$$v^*|_{x=b} = v|_{x=b}-(l+b)\Theta\omega\ \cos\ \omega t \tag{15}$$

$$u^*|_{y=-e}=u|_{y=-e}-e\Theta\omega\ \cos\ \omega t \tag{16}$$

and the amplitude ratio $\xi$ is defined and given as follows:

$$\xi|_{side} = \frac{v^*_{max}|_{x=b}}{b\Theta\omega} = \frac{s_s}{b\Theta}$$

$$= |2+A_1\frac{\pi}{2}\sinh\frac{\pi(y-e)}{2b}-B_1\frac{\pi}{2}\sinh\frac{\pi(H-y)}{2b}| \tag{17}$$

$$\xi|_{bottom} = \frac{u^*_{max}|_{y=-e}}{b\Theta\omega} = \frac{s_b}{b\Theta}$$

$$= |A_1 \frac{\pi}{2}\cos\frac{\pi x}{2b} + B_1\frac{\pi}{2}\cosh\frac{\pi h}{2b}\cos\frac{\pi x}{2b}| \tag{18}$$

An example of the results of calculation is shown in Fig. 7. $s_s/b\Theta$ at $y = -e$ is not zoro because of the first term approximation mentioned above.

In order to observe the motion of the fluid in the tank under rolling condition, some small solid particles were put into the fluid. As seen from Fig. 8, close agreement between observed and calculated values was obtained.

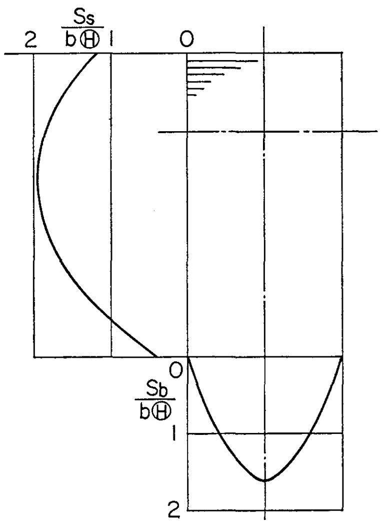


Fig. 7 Fluid velocity at wall

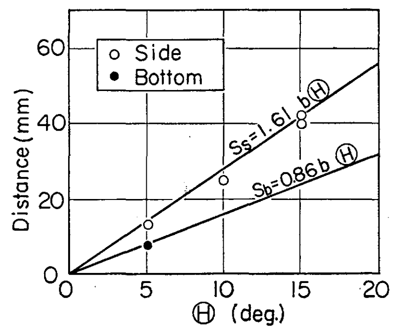


Fig. 8 Comparison with experiment

### 3.4. Rolling effect on heat transfer

Experiments were carried out under three different phases, i.e. cooling, heating and maintaining teperature. But no practical difference was found among the three phases. The rate of temperature change was not so fast under both cooling and heating condition that the state during the test could be regarded as quasi-steady state.

The increment in the Nusselt number by rolling is defined as follows on referring to Eq. (4):

$$\Delta Nu \equiv \Delta \alpha l / \lambda \tag{19}$$

where $l$ is the stiffener space. The Reynolds number is defined as follows for the convenience of the practical use.

$$Re \equiv \frac{u_{wmax} l}{\nu} = \frac{b\Theta\omega l}{\nu} = \frac{2\pi b\Theta l}{T\nu} \tag{20}$$

The effect of the Prandtle number on the heat transfer coefficient is assumed to be a third power analogous to j-factor proposed by A. P. Colburn[5]. Then an empirical formula is derived in the form as follows:

$$\Delta Nu / P_r^{1/3} = CRe^n \tag{21}$$

where $C$ and n are constants determined by experiment.

At the bottom shell plating, heat is transfered by conduction when the ship does not roll and the value of an apparent heat transfer coefficient in this case is usually very small. Therefore, the over-all amount measured can be taken as the increment yielded by rolling. Then the empirical formula for the bottom shell plating is given as follows.

$$Nu / P_r^{1/3} \cong \Delta Nu / Pr^{1/3} = C' Re^{n'} \tag{22}$$

where $C'$ and $n'$ are other constants determined by experiment.

The results of the experiment are shown in Figs. 9 and 10, where physical properties of the fluid are evaluated at the film temperature. The above-mentioned constants were determined from the test results by the least square method and following empirical formulae were obtained.

$$\text{(1) Side} \quad : \quad \Delta Nu = 0.0160 Re^{0.942} Pr^{1/3} \tag{23}$$

$$\text{(2) Bottom} : \quad \Delta Nu \cong 0.0155 Re^{0.910} Pr^{1/3} \tag{24}$$

By the way, in our problems, the Reynolds number defined by Eq. (20) is evaluated to be about $10^3$ at most. Thus the heat transfer from the surface to the fluid closely depends upon the laminar boundary-layer thickness and the theoretical solution Eq. (25) derived by Pohlhausen for this flow circumstance seems to be applicable.

$$Nu = 0.664 Re^{1/2} Pr^{1/3} \tag{25}$$

As an example, we try to apply Eq. (25) to an experiment used ethylene

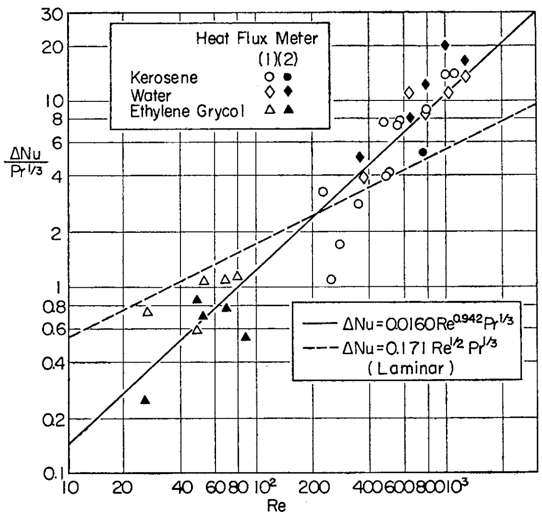


Fig. 9 Increment in heat transfer coefficient by rolling (Side)

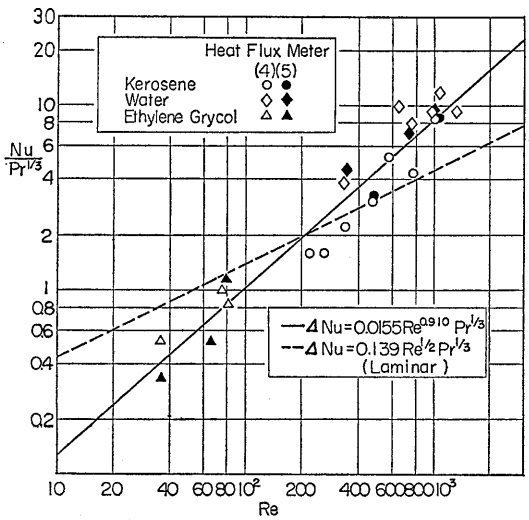


Fig. 10 Increment in heat transfer coefficient by rolling (Bottom)

grycol. In case of $T = 1.43$ sec, the average amplitude ratio at the surface of the side shell plating is calculated by Eq. (17) and the value 0.0662 is obtained. That means

$$u_{max}|_{avr} = 0.0662 b\Theta\omega \qquad (26)$$

Introducing the notation expressed by Eq. (20) and substituting this and Eq. (26) into Eq. (25), we obtain

$$\Delta Nu = 0.171 Re^{1/2} Pr^{1/3} \tag{27}$$

for the heat transfer at the side shell plating. In the same manner as mentioned above, we obtain

$$Nu = 0.139 Re^{1/2} Pr^{1/3} \tag{28}$$

for the bottom shell plating.

Eqs. (27) and (28) are also shown in Figs. 9 and 10 by the broken line, respectively. The coefficients of Eqs. (27) and (28), 0.171 and 0.139, change in fact according to the value of the Reynolds number. Therefore, it is unreasonable to compare Eqs. (27) and (28) with the each experimental results. Moreover, as seen from the figures, it might be said that it is no use trying to obtain empirical formulae in the form

$$Nu \propto Re^{1/2} Pr^{1/3} \tag{29}$$

Therefore, we decide to apply Eqs. (23) and (24) to the analysis of the test results on actual ships.

### 3.5. Velocity profile near the wall

By rolling an empty tank, the velocity of the oscillation of air near the wall was measured with a hot-wire anemometer. Because there is no free surface in this case, the motion of air is different from that of oil as a whole. However, the relative motion of air to the wall would be approximately

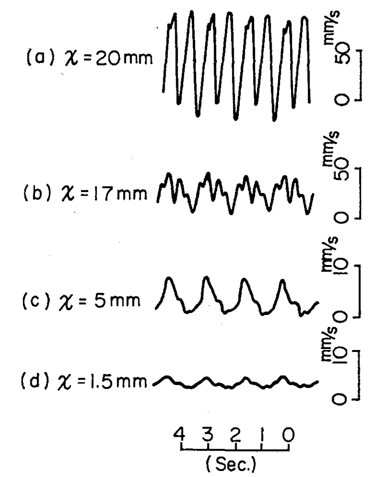


Fig. 11 Variation of flow velocity (T = 1.43 sec)

equivalent to that of oil in case of the same Reynolds number.

The relative velocity of air to the wall was measured in the midst of two stiffeners. Fig. 11 shows the oscillogram, where $\chi$ denotes the distance from the wall. In this case, the Reynolds number calculated by Eq. (20) is 142. Fig. 11 (a) shows the velocity at the slight outside of the edge of stiffeners. The velocity of air changes sinusoidally in obedience to the motion of the tank. Fig. 11 (b) shows the velocity at the slight inside of the edge of stiffeners, where fluctuations of higher frequency than that of rolling are observed. This phenomenon must be due to eddies from the edge. Figs. 11 (c) and (d) show the fluctuations at the referred positions, respectively. The absolute value of the velocity is so small that the influence of natural convection caused by the hot-wire anemometer itself can not be neglected. One should note that the scale of (c) and (d) is five times as large as that of (a) and (b).

The profile of the maximum velocity versus the distance from the wall is shown in Fig. 12. As seen from the figure, the velocity amplitude decreases suddenly at inside of the edge of stiffeners.

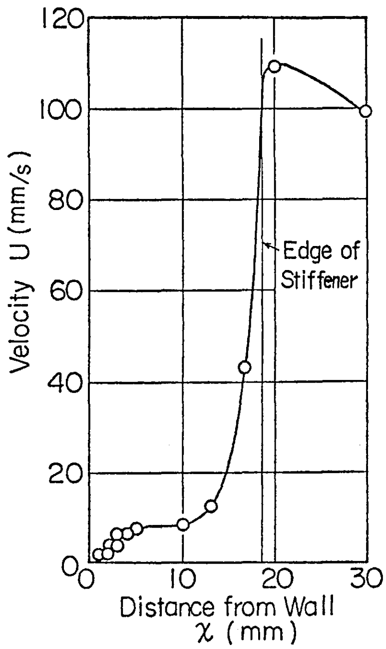


Fig. 12 Velocity profile

## 4. Analysis of Data of Test Ship

The test results of actual ship were also analyzed considering above-mentioned rolling effect.

### 4.1. Outline of the test on actual ship

A series of tests concerning the heat losses from the cargo tank and the heat transfer from the heating coil during tank heating were carried out on an actual oil tanker in March 1968 by the 102 Research Committee of Shipbuilding Research Association of Japan, and one of the authors took charge of the test.

Tests were carried out under the following conditions:

Test Ship: 33,000 DWT Oil tanker

($L \times B \times D = 192.3$ m $\times 26.8$ m $\times 13.7$ m)

Table 3 Characteristics of Oil

| Oil | $\theta$ (°C) | $\rho$ (kg/m³) | Cp (kcal/kg°C) | $\lambda$ (kcal/mh°C) | $\nu$ (m²/s) |
|---|---|---|---|---|---|
| Kalimatan Crude | 50 | 869 | 0.520 | 0.132 | $259\times10^{-6}$ |
| | 60 | 862 | 0.531 | 0.132 | 57 |
| | 70 | 854 | 0.544 | 0.132 | 33 |
| Bachequero Crude | 30 | 965 | 0.470 | 0.108 | 2700 |
| | 40 | 959 | 0.482 | 0.108 | 1200 |
| | 50 | 953 | 0.496 | 0.107 | 620 |
| | 60 | 947 | 0.508 | 0.107 | 350 |
| | 70 | 941 | 0.521 | 0.106 | 210 |
| C-Heavy Oil | 30 | 985 | 0.430 | 0.101 | 2090 |
| C-Heavy Oil | 30 | 950 | 0.440 | 0.104 | 5720 |
| B-Heavy Oil | 30 | 900 | 0.445 | 0.106 | 140 |

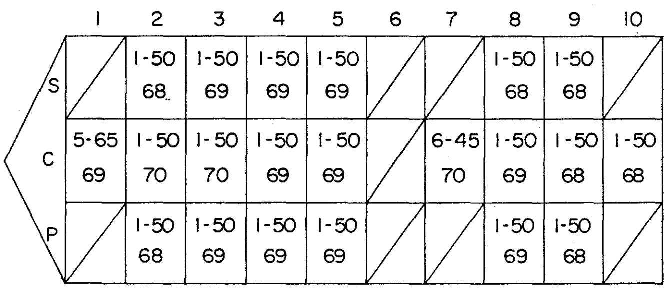


Upp. Line : Sounding Depth (m-cm)
Low. Line : Initial Temperature (°C)

Fig. 13 Stowage condition

Ship's Course: From Balikpapan (Indonesia) to Negishi (Japan)
Characteristics of Crude Oil: See Table 3
Stowage Condition: See Fig. 13

The temperature of the plating, such as the side shell, the bottom shell, the deck and the bulkhead, and the temperature distribution in the cargo oil and that on the heating coil and so on, were measured mainly in the No. 5 port side tank and totally at 75 points with sheathed thermocouple. The heat flux through the plating was also measured at 11 points in the above-mentioned tank with the heat flux meter designed and manufactured by one of the authors.

The test, which was of 8 days duration, consisted of two phases, that is the cooling and the heating. Readings of the temperature and the heat flux were taken every two hours, but records themselves were recorded on oscillographs automatically and continuously throughout the test duration.

### 4.2. Test results

(1) Temperature distribution in cargo oil

Test results are shown in Figs. 14 and 15. As seen from the figures the temperature of the cargo oil is almost uniform only except the thin layer near the shell plating. Especially above the heating coil, the temperature difference in the oil in the direction of the depth was very small and did not exceed 1 °C. This fact differs very much from the test results of a large size model tank settled on land[6]. And this difference comes evidently from the stirring effect by rolling of ship.

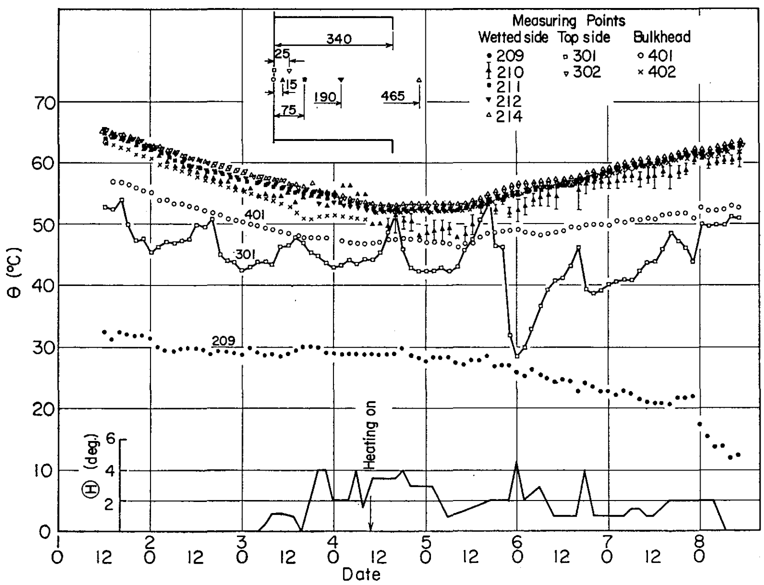


Fig. 14 Temperature history (Side)

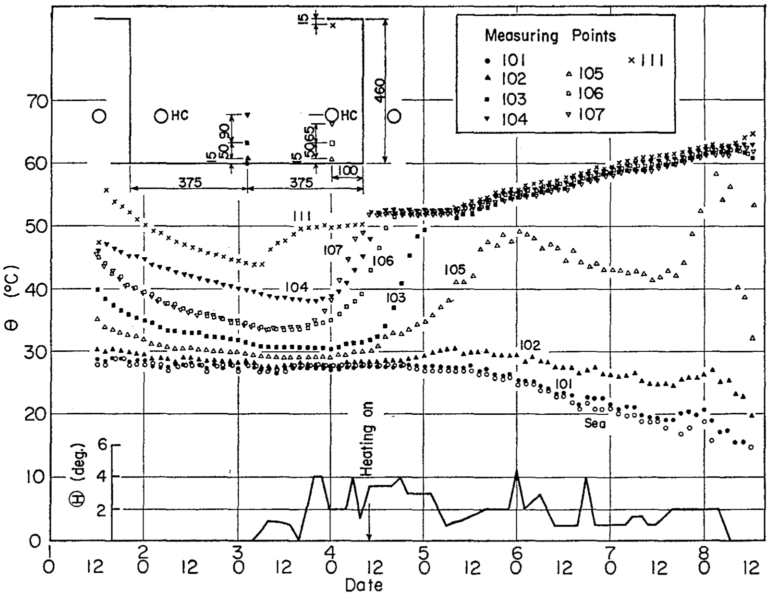


Fig. 15 Temperature history (Bottom)

(a) Temperature distribution in the center of tank

As shown in Fig. 14, the temperature of the oil inside of the measuring point No. 211, which is located at the distance of 75 mm from the side shell plating, shows the uniformity within the difference of 1 °C throughout the duration of test. This phenomenon has been confirmed in the other tests on ship.[2]

(b) Temperature distribution in the neighbourhood of shell plating

As shown in Fig. 14, the temperature at the measuring point No. 210, which is located at the distance of 15 mm from the side shell plating shows a little lower value than those at the inner points and remarkable cyclical fluctuation within the range of about 5 °C in the heating phase. This fluctuation is not observed during the cruising in very calm tropical sea where the rolling of ship was almost negligible.

Temperatures at the inner points No. 302 and No. 211, for example, show little deviation from that of the center of tank, in spite of the great difference in the position, that is, the former is located 25 mm from the wetted-side plating and the latter 75 mm from the top-side plating.

The fluctuation mentioned above is also observed and mentioned in another paper.[3] It is not confirmed in our test that if the period of the fluctuation corresponds to that of rolling of ship or not, because the sampling rate of temperature is once in every 90 seconds and too large in comparison with rolling period, but it is obvious that the fluctuation is caused by the stirring effect of rolling of ship.

(c) Temperature distribution in the neighbourhood of bottom plating

As shown in Fig. 15, a remarkable difference is observed between the cooling and the heating phase.

The temperature distribution in the cooling phase shows the same pattern of heat conduction in solids, because the cargo oil has such a high fluidity point as 47.5 °C. Especially, it is clear that in the initial stage of the test when the ship does not roll, heat conduction is dominant at the bottom shell plating, even though the temperature of cargo oil is higher than its fluidity point.

The oil temperature near the bottom shell plating shows rise before the start of heating. As seen from Fig. 15, the beginning of the oil temperature rise corresponds to the start of rolling of ship. Therefore, it is clear that this phenomenon originates in the stirring effect of rolling of ship. Moreover, it is worth noting that the stirring effect prevails to the region where the temperature of oil is far below its fluidity point.

In the heating phase, the temperature at the points No. 102 and No. 105, both of which are at the distance of 15 mm from the bottom shell plating, show considerably lower values than those at the points No. 103 and No. 106, both of which are at the distance of 65 mm from the bottom shell plating and whose tempertures and that of the center of tank are almost identical. The position of the heating coil is 150 mm above the bottom shell plating and the thermal diffusion in the oil below the heating coil may be little. So, such an uniformity in the oil temperature must have been achieved by rolling of ship. That means the existence of the fluid motion, as expected by the consideration in paragraph 3. 3.. The so-called stationary layer seems to be considerably thinner under rolling condition.

(2) Heat flux through shell plating

Test results are shown in Fig. 16.

(a) Heat flux through top-side plating

The Heat flux shows fundamentally a parallel change to the bulk temperature of the cargo oil, and the periodic change whose period is one day is superposed upon this. That is, the heat flux decreases from noon to evening because of the direct exposure to the sun and it increases in the night.

The heat flux through the top-side plating varies much more violently than that through the wetted side plating. This phenomenon seems to be closely related to the distribution of the flow velocity at the surface of plating, as mentioned in paragraph 3. 3.. Moreover, the range of the heat flux variation seems to have the tendency that that becomes larger when the viscosity of oil becomes lower following the raise of its temperature.

(b) Heat flux through wetted-side plating

As shown in Fig. 16, the heat flux changes almost parallelly to the change of the bulk oil temperature and shows a distinct jump at start of rolling. The jump such as this has not been observed in the other test. [1)~3)]

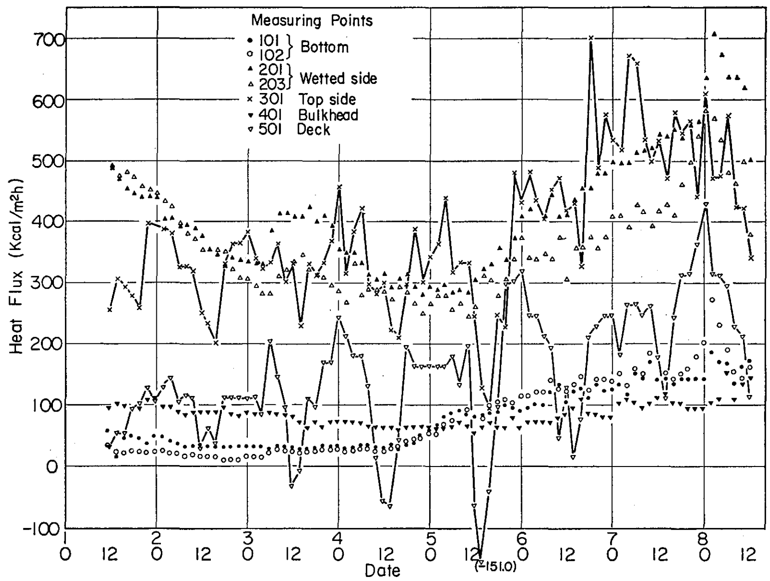


Fig. 16 History of heat flux

(c) Heat flux through bottom plating

The heat flux was measured at two points, one of which was just below the heating coil and the other was the center of the longitudinal frame space.

Test results are shown also in Fig. 16. There is a slight difference between the two results of measurement.

In the cooling phase, the former shows a little larger value than the latter, but they correspond exactly to the respective local temperature gradient recorded. Therefore, there is no contradiction so far as the test data are concerned. Both results can be reasonably explained as heat conduction in solids.

In the heating phase, the former shows lower value than the latter. This phenomenon is closely related to the motion of the cargo oil induced by rolling. That is, as mentioned in paragraph 3. 3., the velocity of flow does not distribute uniformly in the longitudinal frame space, and it is larger at the center than at the edge. Therefore, it is expected that the stationary layer, if it exists, will be the thinnest at the center of the frame space. The temperature records shown in Fig. 15 verify this fact.

A typical example of the rolling effect is seen in the paper concerning to the fuel oil heating. [3] In the case, the rolling effect appears very evidently, because of the extremely low viscosity of the tested oil. According to the paper, the stationary layer at the bottom vanished completely and the heat flux showed very large value of 200 kcal/m$^2$h. Such a large value cannot be expected by the heat conduction only, and it is clear that the heat transfer is affected by the forced convection due to rolling of ship.

## 4.3. Analysis of the test results and investigation

(1) Side plating

Analyzed results of the heat transfer coefficient (we term it "$\alpha$-value" hereafter) and the overall heat transfer coefficient (we term it "K-value" hereafter) are shown in Figs. 17 and 18.

Considering the fluidity point of the tested cargo oil, reference temperature is defined as follows:

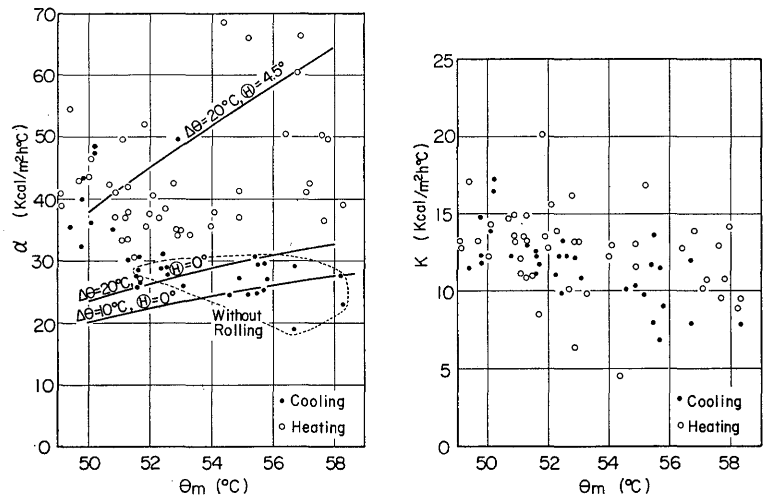


(a) $\alpha$-value (b) K-value

Fig. 17 Heat transfer (Top side)

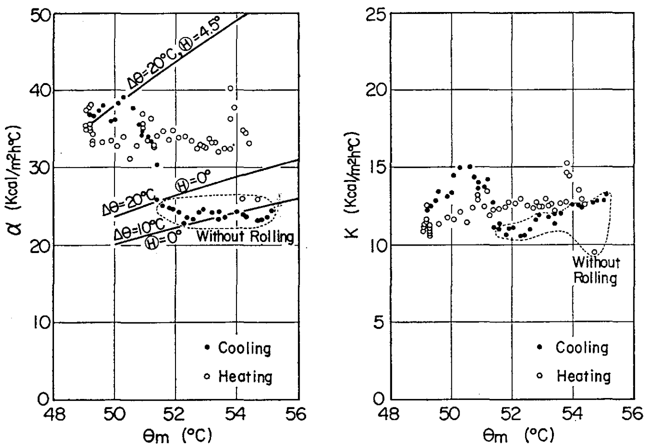


(a) $\alpha$-value (b) K-value

Fig. 18 Heat transfer (Wetted side)

$$\theta_m = \{max(\theta_h, 45.0) + \theta_f\}/2 \tag{30}$$

By using this reference temperature, the $\alpha$-value at the surface of the solidification layer is also expressed by Eq. (5).

In general, the K-value is expected to be almost the same as the $\alpha$-value for the side plating. But, as shown in the abovementioned figures, there is a great difference between the two. This fact depends on the existence of the solidification layer of wax contained in the cargo oil, as to be mentioned later.

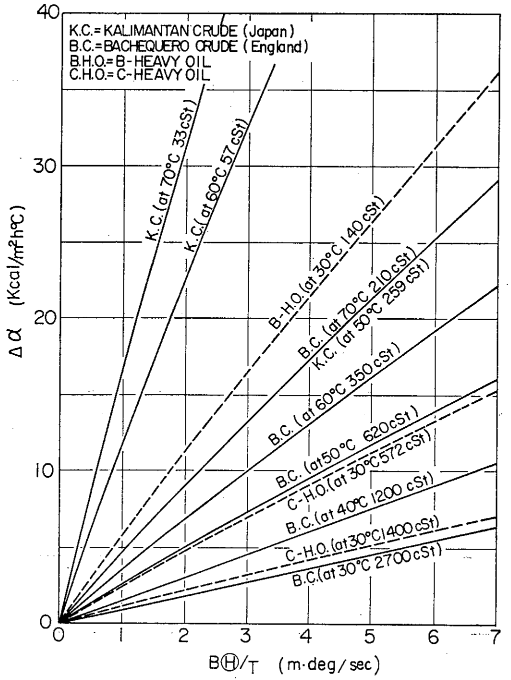

Fig. 19 Increment in heat transfer by rolling (Side)

The increment of the heat transfer coefficient calculated by Eq. (23) is shown in Fig. 19 and properties used in the calculation are tabulated in Table 3. The maximum value of the parameter $B\Theta/T$ is 3.3 m deg/sec (because $B = 7.4$ m, $\Theta = 4.5$ deg, $T = 10$ sec) for the actual ship test. Therefore, $\Delta\alpha$ is estimated to be 33.5 and 14.5 kcal/m$^2$h°C for $\theta = 60$ and 50 °C, respectively. And these values are almost the same as the $\alpha$-value calculated by Eq. (5).

When the $K$-value is analyzed for the side shell plating, the $\alpha$-value on the outer surface must be evaluated considering forced convection and radiation. Evaluation of those values were made by applying following equations:

For forced convection

$$\frac{\alpha_c l}{\lambda} \equiv Nu = 0.036\ Re^{4/5} Pr^{1/3} \quad \text{(Colburn's equation)} \tag{31}$$

For radiation

$$\alpha_r = 4.88\times10^{-8}\varepsilon_r\{\theta_h+273)^4-(\theta_a+273)^4\}/(\theta_h-\theta_a) \tag{32}$$

where $\varepsilon_r$ : Emissivity of the plating (−)
$\theta_h$ : Temperature of the plating (°C)
$\theta_a$ : Temperature of atomosphere (°C)

Moreover, sometimes the thermal resistance of the solidification layer becomes a problem in analyzing the K-value. The thermal resistance of the solifidification layer of the tested cago oil is calculated to be $0.73\times10^{-2}$ m²h °C/kcal per 1 mm in thickness.

Thus, the K-value for the side shell plating is summarized as follows:

For the top side

$$K = 1/\{1/(\alpha+\Delta\alpha)+1/(\alpha_c+\alpha_r)\} \tag{33}$$

For the wetted side

$$K = \alpha+\Delta\alpha \tag{34}$$

The influence of the solidification layer should be considered, when it exists. But the thermal resistance of the sea water side surface is almost always negligible in comparison with those of the factors mentioned above.

(a) Top side

The $\alpha$-value for the inner surface is shown in Fig. 17(a). The lower curve in the figure is the calculation by Eq. (5) and the upper one is that including the increment by rolling expressed by Eq. (23). As seen from the figure, the measured values almost agree with the calculated ones.

The K-value is shown in Fig. 17(b).

Roughly speaking, lower values and higher values in the figures are correspond to the measured values obtained during sunshine and in the duration of larger rolling angle, respectively. In regard to the mean value during the night, $\alpha+\Delta\alpha$ is roughly estimated as 50 kcal/m²h°C according to Fig. 17(a) and $\alpha_c$ and $\alpha_r$ as 18 and 2 kcal/m²h°C by Eqs. (31) and (32), respectively. Therefore, corresponding K-value is estimated as 14.3 kcal/m²h°C. The experimental value which corresponds this situation is estimated 14 kcal/m²h°C from Fig. 17(b). The difference between the above two is due to the existence of the solidification layer, and its thickness is calculated as 0.2 mm. Similarly, the thickness in the cooling phase with no rolling is calculated as 1.2 mm.

These values are reasonably acceptable in the light of the oil temperature distribution near the shell plating.

(b) Wetted side

Results are shown in Figs. 18 (a) and (b) in the same manner as Fig. 17. As seen from the figures, the fact that the scatter of data is considerably smaller than that shown in Fig. 17, means the more thermally stable condition in the region. Experimental values agree well with the calculated ones.

The thickness of the solidification layer is calculated as tabulated in Table 4. It shows the tendency of increase in the cooling and decrease in the heating phase.

A very large K-value such as 25 kcal/m$^2$h°C has been reported in the results of the test carried out in England.[2] The rolling angle in this case is analyzed to be about 18 degree using Eqs. (5) and (23). This value seems to be compatible with the description of "violent rolling" in the paper.

(2) Bottom plating

Results are shown in Fig. 20.

Table 4 Change in the thickness of solidification layer (Wetted side)

| | | $\theta$m (°C) | $\alpha_h$ (kcal/m$^2$h°C) | K (kcal/m$^2$h°C) | d (mm) |
|---|---|---|---|---|---|
| Cooling Phase | without Rolling | 55.0 | 23.5 | 12.8 | 4.9 |
| | | 51.6 | 25.0 | 11.0 | 7.0 |
| | with Rolling | 49.2 | 36.9 | 12.2 | 7.5 |
| Heating Phase | | 49.1 | 35.2 | 11.2 | 8.3 |
| | | 52.1 | 34.0 | 12.6 | 6.8 |
| | | 54.4 | 33.2 | 12.5 | 6.8 |

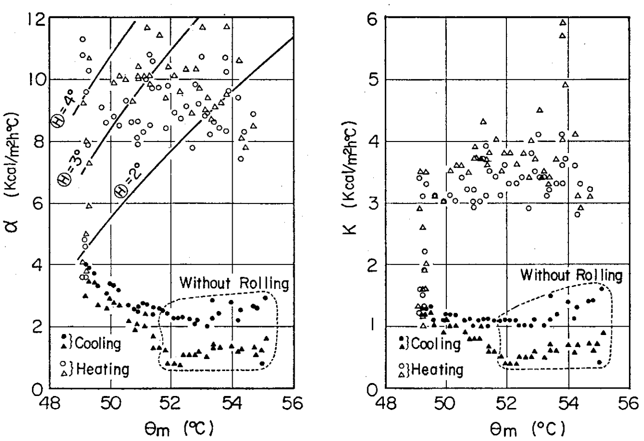


(a) $\alpha$-value (b) K-value

Fig. 20 Heat transfer (Bottom) (Considering solidification layer)

Three patterns of the heat transfer are considered: the heat conduction both in the cooling and in the heating phase with no rolling and the heat transfer by forced convection with rolling.

(a) Conduction in cooling phase with no rolling

The $\alpha$-value for the inner surface is given as follows:

$$\alpha = \{\lambda C_p \rho / (\pi t)\}^{1/2} \tag{35}$$

The value of $(\lambda C_p \rho)$ does not change much by kinds of oil and the $\alpha$-value is approximated to be about 1 kcal/m$^2$h°C, except the beginning of cooling.

(b) Conduction in heating phase with no rolling

A so-called stationary layer is formed below the heating coil and the $\alpha$-value is expressed by $\lambda/d$. Where $d$ is the distance between the heating coil and the bottom shell plating. The $\alpha$-value is estimated about 0.137/14 $\doteqdot$1 kcal/m$^2$h°C.

Both values mentioned above are almost identical. Therefore, it is expected that they yield the same K-value in case of the non-rolling condition regardless of heating.

In the test on an actual ship, heat conduction at the bottom shell plating with no rolling is evidently dominated by heat conduction as seen from Fig. 15. The K-value takes, as shown in Fig. 20(b), the value between 0.5 and 1.5 kcal/m$^2$h°C and decreases according to the fall in the bulk temperature. These results agree approximately with calculated ones by Eq. (35).

(c) Convection under rolling

The $\alpha$-value is evaluated by Eq. (24). Test results and calculated ones are shown in Fig. 20(a).

As seen from the figure, data are mostly distributed in the region bounded by $\Theta = 2$ and 4 degree and agree well with the calculated results.

An extremely large value such as 13.3 kcal/m$^2$h°C was reported in a paper.[3] But the corresponding rolling angle is calculated as only 1.2 degree by Eq. (24) because of the very low viscosity of the tested oil. Therefore, the large K-value mentioned above does not contradict to the fact that it was obtained during the sea trial test in the calm sea.

## 5. Conclusion

(1) Increment in the heat transfer coefficient for the shell plating by rolling of ship was experimentally investigated and the following empirical formulae were obtained:

For side shell plating: $\Delta Nu = 0.0160\ Re^{0.942} Pr^{1/3}$

For bottom shell plating: $\Delta Nu \cong 0.0155\ Re^{0.910} Pr^{1/3}$

(2) The experimental results obtained by the test on an actual ship are reasonably and well explained using the empirical formulae mentioned above.

(3) Increment in heat transfer by rolling of ship is mainly caused by stirring effect of stiffeners.

**Appendix: Heat flux meter**

As shown by Fourier's Law for Heat Conduction, when heat flows through a plate, it can be measured by knowing temperature difference between two surfaces of the plate.

The heat flux meter used in our tests is the foil type meter which detects the temperature difference between both surfaces of the base plate. To improve the accuracy of the heat flux meter, the following considerations were taken:

(1) Laminated epoxy glass sheet of 0.5 mm in thickness were used to reduce thermal resistance so that the heat flow will not be disturbed.

(2) In order to detect accurately the temperature difference between both surfaces of the base plate, the print wiring method were applied. In order to obtain magnification of detection, a thermopile system was used.

(3) Characteristics of the heat flux meter such as the response speed and the error caused by heat conduction in thermocouples were theoretically examined.

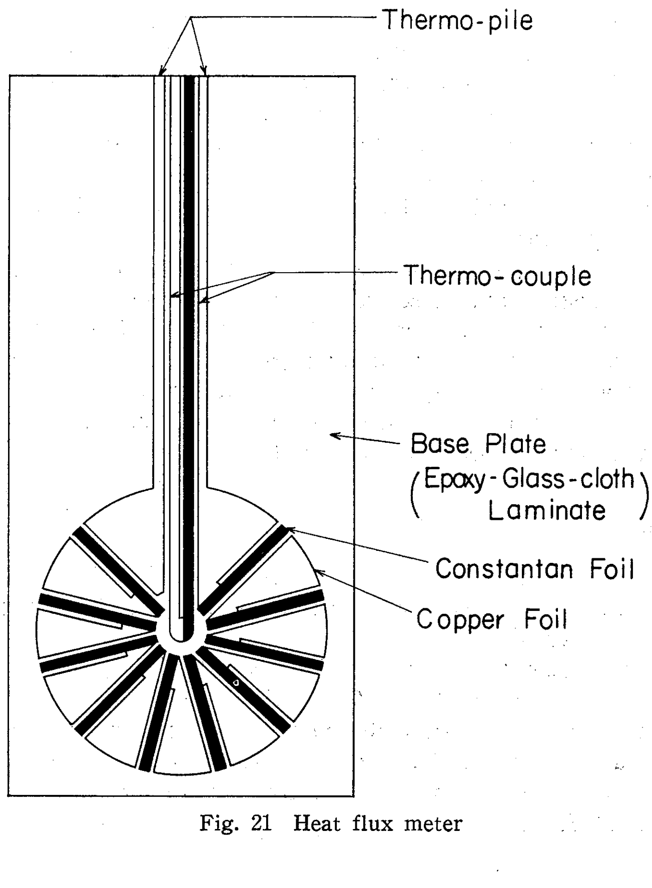


Fig. 21 Heat flux meter

Calibration of the heat flux meter was carried out by means of the comparison method with pure copper and so on. Following empirical formula of the thermal conductivity of the base plate was obtained for the temperature range between -100 °C and 70 °C.

$$\lambda_{HFM} = 0.30 + 0.0008\ \theta \quad \mathrm{kcal/mh^{\circ}C}$$

Therefore, the thermal resistance of the heat flux meter is calculated as $1.47 \times 10^{-2} \mathrm{m^2\ h^{\circ}C/kcal}$ at 50 °C.

A pattern of the heat flux meter used in the experiment on the ship is illustrated in Fig. 21.

**Notation**

| | | |
|---|---|---|
| A | : area | ($m^2$) |
| B | : width of tank | (m) |
| b | : half width of tank | (m) |
| C | : constant | (−) |
| $C_p$ | : specific heat | (kcal/kg°C) |
| d | : thickness of stiffener | (m) |
| e | : distance | (m) |
| g | : acceleration of gravity | ($m/sec^2$) |
| H | : distance | (m) |
| h | : H - e | (m) |
| K | : overall heat transfer coefficient | ($kcal/m^2h^{\circ}C$) |
| k | : height of stiffener | (m) |
| l | : length | (m) |
| n | : constant | (−) |
| Q | : heat flow rate | (kcal/h) |
| s | : amplitude of rolling | (m) |
| T | : period of rolling | (sec) |
| t | : time | (h) |
| u | : velocity | (m/sec) |
| x | : coordinate | (−) |
| y | : coordinate | (−) |
| $\alpha$ | : heat transfer coefficient | ($kcal/m^2h^{\circ}C$) |
| $\Delta\alpha$ | : increment of $\alpha$ by rolling | ($kcal/m^2h^{\circ}C$) |
| $\Theta$ | : angle of rolling | (rad, deg (in Fig. 19)) |
| $\theta$ | : temperature | (°C) |
| $\lambda$ | : coefficient of thermal conductivity | (kcal/mh°C) |
| $\nu$ | : coefficient of kinematic viscosity | ($m^2/h$) |
| $\xi$ | : magnification factor of rolling angle | (−) |
| $\phi$ | : fin efficiency | (−) |
| $\Psi$ | : apparent fin efficiency | (−) |
| $\omega$ | : angle velocity | (rad/sec) |
| Nu | : Nusselt number | (−) |
| Gr | : Grashoff number | (−) |
| Pr | : Prandtle number | (−) |
| Re | : Reynolds number | (−) |

### Suffixes

$\infty$ : at infinity
a : air
c : convection
f : fin
h : hull plate
r : radiation
w : wall

### References

1) Van Der Heeden, D. J., Heat-Transfer in Cargotanks of a 50,000 DWT Tanker, Netherlands Ship Research Center TNO, Report No. 67S, 1965.
2) Saunders, R. J., Heat Losses from Oil Tanker Cargoes, Trans. I. Mar. E., Vol. 79, No. 12, 1967.
3) Van Der Heeden, D. J., Experimental Evaluation of Heat Transfer in a Dry-Cargo Ships' Tank, Using Thermal Oil as a Heat Transfer Medium, Netherlands Ship Research Center TNO, Report No. 111 M, 1968.
4) Tamiya, M., On the Dynamical Effect of Free Water Surface, J. N. S. A. Japan, Vol. 103, 1958. (in Japanese)
5) Colburn, A. P., Trans. A. I. Ch. E., Vol. 29, 1933.
6) Couchman, A. A. J., Heating of High-viscosity Oil Cargoes, Trans. I. Mar. E., Vol. 78, 1966.

(Received April 26, 1976).